Chapter 7

Resolving Power & Efficiency

In this chapter the resolution and efficiency of the spectrograph is investigated and estimates of the required exposure times are made for various astronomical objects.

7.1 System Resolving Power

The resolving power of a spectrograph at some wavelength, λ, is defined as that wavelength divided by the smallest separation, $\Delta\lambda$, between two monochromatic wavelengths, λ and $\lambda + \Delta\lambda$, whose images are just resolvable. This may sound simple, but in practice the resolving power (or resolution if you prefer) may be limited by one of a variety of factors.

In the case of diffraction limited systems (but not here) the Raleigh limit is most commonly used. In practical terms, this corresponds to a central minimum between two adjacent peaks of. less than 80% of the amplitude of the peaks.

For a sampling detector (i.e. a detector with pixels), such as the CCD, a further restriction is placed by the Nyquist sampling criterion. This represents an absolute maximum spatial resolution on the detector of 2 pixels. For spectrographs like the UES / AAT echelle spectrograph [Walker and Diego, 1985] this is relevant because the projected slit width (not a fibre fed system) is matched to two detector pixels giving:

$$R = \frac{d}{\lambda_{max}} \frac{width_{det}}{width_{pixel}} \cos\theta \sin\theta_b \cos\gamma \tag{7.1}$$

Applying this formulae to our spectrograph gives $R \approx 20,000$, however, the image of the fibre is in the order of 4 pixels wide (2×2 binning of the CCD pixels is beyond the scope of this paper and will be investigated at a later date) so this value is somewhat optimistic.

In this spectrograph neither of the previously mentioned methods of determining the resolving power are directly applicable. The calculations are therefore done from first principals using the same criterion as the Raleigh limit. The additional condition that the minimum must be less than 80% of the amplitude of the smaller of the two peaks allows for differing spectral line strengths. The effect of focussing errors is also included.

The grating equation can be written as:

$$\lambda = \frac{d}{m}\left[\sin\left(\theta_b\right) + \sin\left(\theta_b - \theta_r\right)\right]\cos\gamma \tag{7.2}$$

and differentiated to give:

$$\frac{\delta\lambda}{\delta\theta_r} = \frac{d}{m}\cos\left(\theta_b - \theta_r\right)\cos\gamma \tag{7.3}$$

Because the angle of dispersion is much smaller than the blaze angle, then it is sufficient to calculate the resolution or resolving power only at the blaze peak. The resolving power of the spectrograph is then:

$$\frac{\lambda}{\delta\lambda} = \frac{2\tan\theta_b}{\delta\theta_r} = \frac{2F_k\tan\theta_b}{D} \tag{7.4}$$

where D is the minimum separation between peaks at the detector. Although D can be derived analytically (with a great deal of difficulty), a numerical method was chosen.

First a profile of the fibre image (in the dispersion direction) was calculated. Figure 7.1 shows the change in profile for various values of $\varepsilon = \varepsilon_{cam} = \varepsilon_{coll}$ clearly illustrating spreading of the image as the amount of error increases.

In order to measure the minimum separation between peaks, a given profile is added to itself with an offset of distance D. The combined profile is then “binned" into 12μ wide pixels. This is then repeated until a minimum value of D is found for which the above resolution criterion is met. Results are shown in Figure 7.2.

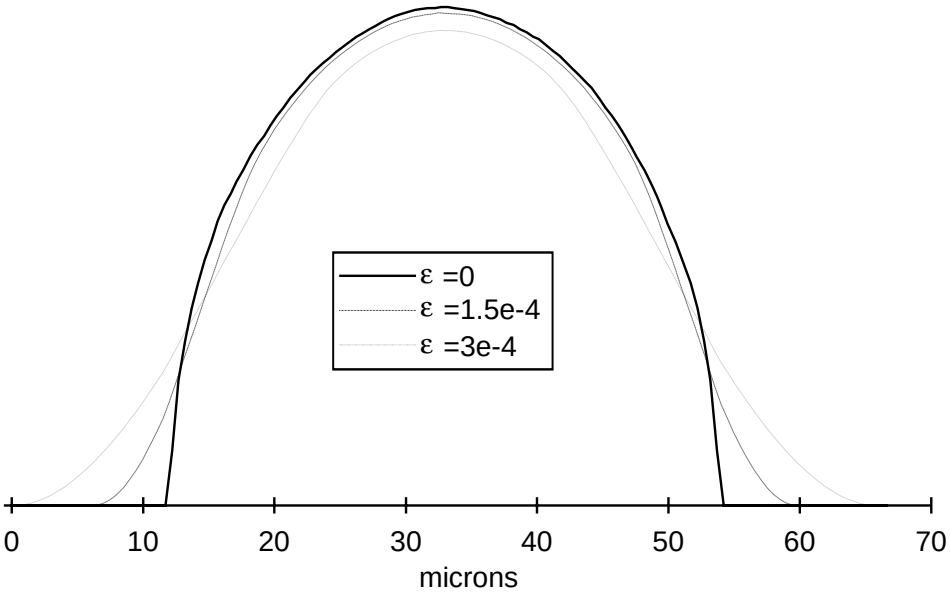

Figure 7.1: Profile of the fibre image in the dispersion direction.

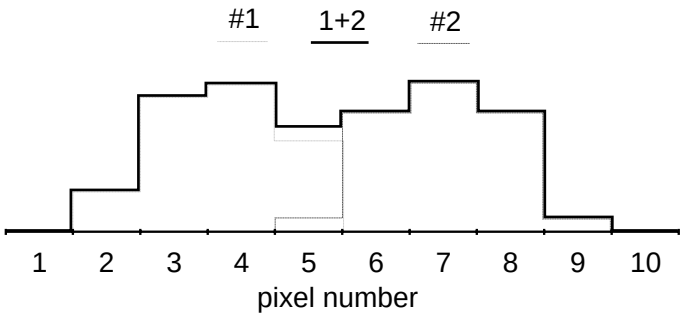

Figure 7.2: “Binned", overlapping profiles with a separation slightly greater than required for resolvability.

On the assumption that both the collimator and camera lenses will be adjusted for optimum performance at the same wavelengths, it is not unreasonable to assume that $\varepsilon_{cam} \approx \varepsilon_{coll}$ $(= \varepsilon)$. Figure 7.3 shows minimum separations found for a number of error values with varying ratios between the two peak intensities.

Although the minimum separation varies significantly with the ratio of the peak sizes, the collimator and camera errors have relatively little effect.

By placing numerical values in equation 7.4 the resolving power of the

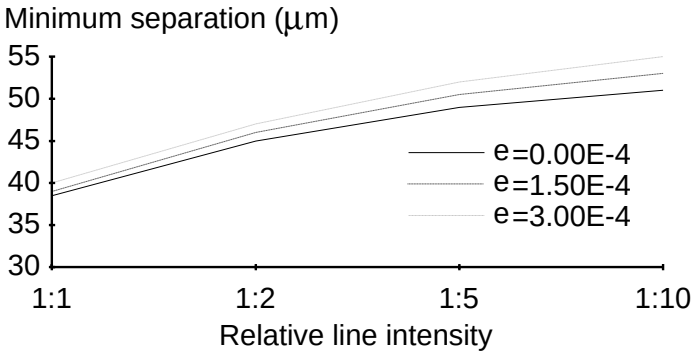

Figure 7.3: Resultant minimum separations.

spectrograph can be calculated for the range of expected error values with varying ratios between the two peak intensities. This is shown in Figure 7.4.

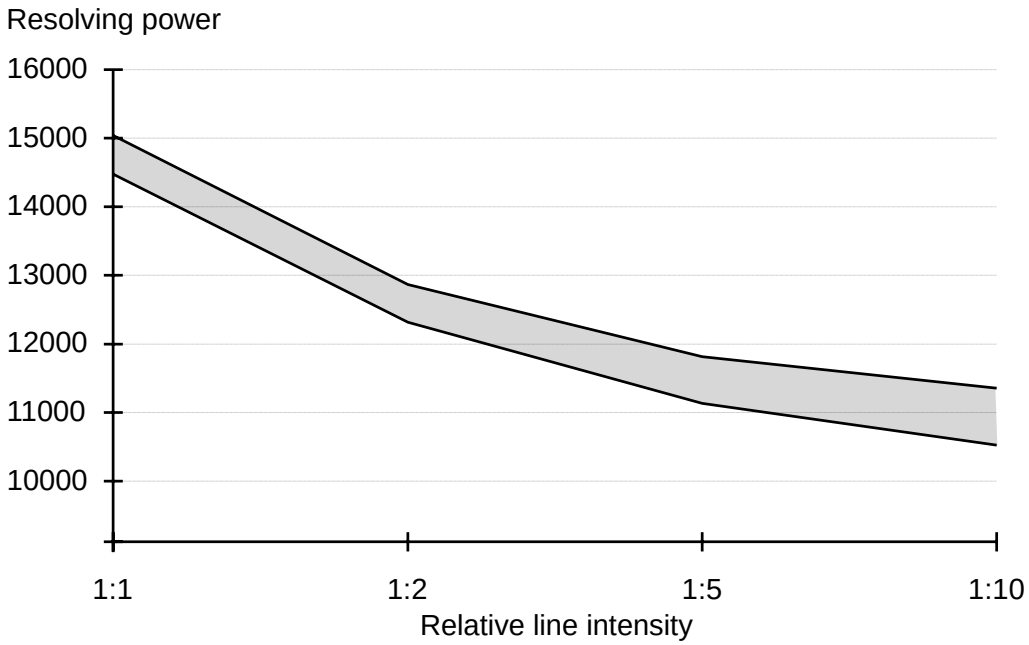

Figure 7.4: Resolving power of the UQ echelle spectrograph.

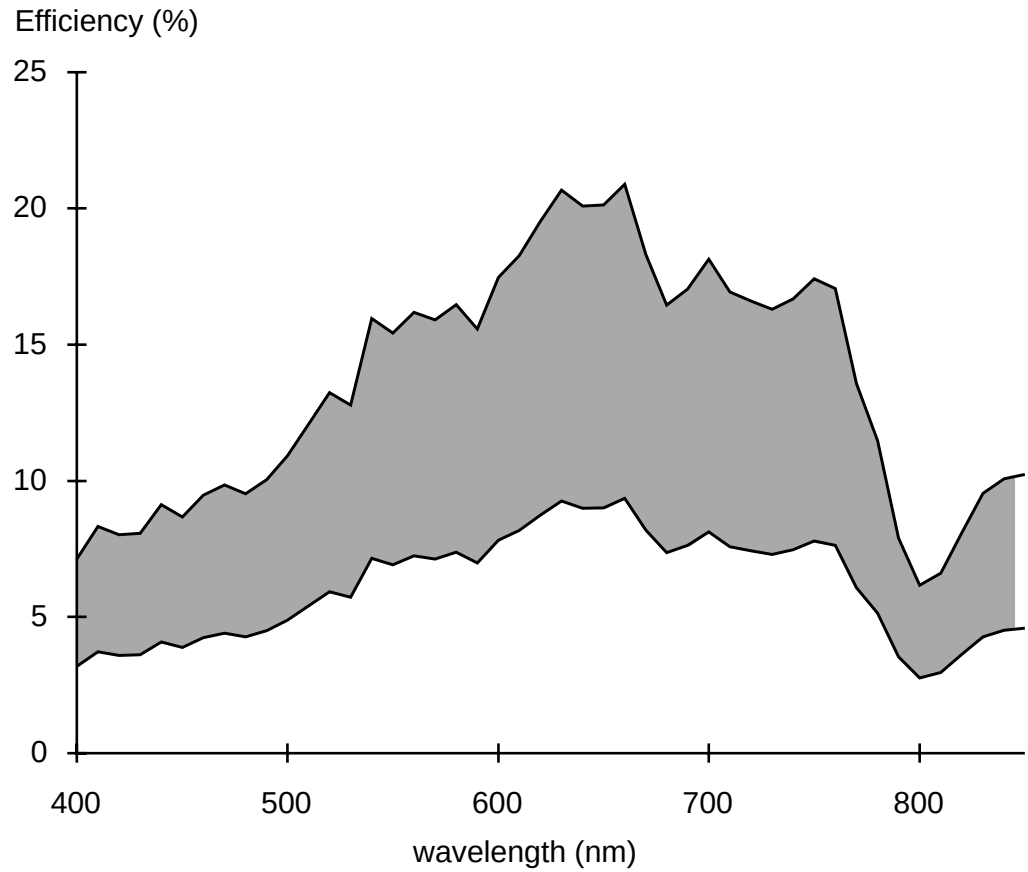

Figure 7.5: Efficiency with a f-10 beam entering the optical fibre. The range of values shown is due to the variation in efficiency in each spectral order with the maximum corresponding to wavelengths at the blaze peak.

7.2 System efficiency

The efficiency of the complete system, illustrated in Figure 7.5, is found by taking the product of the through-puts for each individual component. These were found in Chapters 3 to 6. In order to avoid complications caused by differing telescope focal ratios, a value of f-10.0 was assumed.

For input beams faster than f-10 the efficiency is reduced due to focal ratio degradation in the optical fibre link. If this is the case then the actual efficiency = efficiency(f-10)$\times C_{FRD}$. Based on the data from chapter 3, C_{FRD} is shown in Figure 7.6.

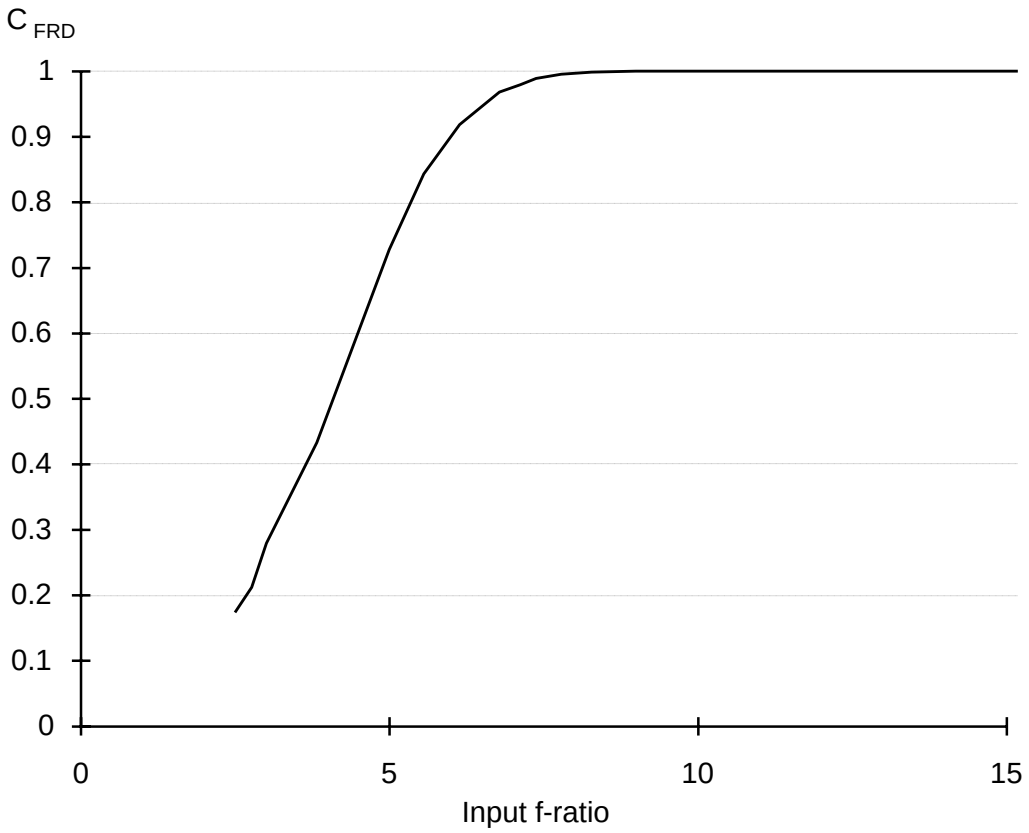

Figure 7.6: Efficiency multiplying factor, C_{FRD}, as a function of input focal ratio.

7.3 Exposure times

The exposure time for any given object is dependant on a large number of factors such as the spectral distribution and intensity of the object under observation, aperture and focal ratio of the telescope being used, and of course the characteristics of the spectrograph (including detector saturation levels, etc..). The smallest time is determined by the signal to noise ratio (SNR). Considering the variation in efficiency (see Figure 7.5), a SNR of greater than 100:1 at the point of maximum sensitivity was considered to be the minimum requirement. The largest exposure time is just less than the time required for the CCD detector pixels to reach saturation.

In order to determine the required exposure times and the limiting magnitudes (magnitude of the dimmest object that can be observed) the number

and rate of electrons generated in the CCD pixels by light (or more exactly photons) from the object being observed must be found. Taking into account the spectrograph efficiency, ε, the electron density in the detector, N, for n photons with a wavelength range of λ to $\lambda + \Delta\lambda$ entering the optical fibre link is:

$$N_{det}(\lambda) = \frac{n(\lambda)}{a_{det}(\lambda)} \times \varepsilon_{spect}(\lambda) \times C_{FRD} \tag{7.5}$$

where

$$a_{det} = \frac{\pi F_k^2 \tan\theta_b}{\lambda F_c} \times \Delta\lambda \times r_f \tag{7.6}$$

(A more detailed derivation of this and following equations is found in Appendix C)

The spectral distribution of the light from a star can be approximated fairly well using the star's effective surface temperature with "black body" radiation curves. Using the Planck equation, the fraction of the energy emitted in a wavelength range of λ to $\lambda + \Delta\lambda$ is:

$$E_{ref}(\lambda, T) = \frac{15}{\pi^4 \lambda^5} \left(\frac{hc}{kT}\right)^4 \frac{\Delta\lambda}{\left(e^{\frac{hc}{\lambda kT}} - 1\right)} \tag{7.7}$$

Energy from the sun arriving at the top of the earths atmosphere, L_{sun}, is 1350 $\mathrm{J/sec/m^2}$. This corresponds to an apparent bolometric magnitude, m_{bol}, of -26.9. Therefore at $m_{bol} = 0$:

$$L_0 = L_{sun} 10^{\left(\frac{m_{bol,sun}}{2.5}\right)} = 24 \times 10^{-9} \mathrm{J/sec/m^2} \tag{7.8}$$

On the assumption that atmospheric absorption is negligible then the number of photons entering a telescope of aperture A can be calculated for a star with an apparent bolometric magnitude, m_{bol}, and an effective surface temperature, T.

$$n_{star}(\lambda, T) = 10^{\left(\frac{m_{bol,sun}}{2.5}\right)} L_0 E_{ref}(\lambda, T) \frac{\lambda}{hc} \frac{\pi A^2}{4} \mathrm{photons/sec} \tag{7.9}$$

then the number of electrons generated in a single pixel is::

$$N_{pixel}(\lambda) = 10^{(\frac{m_{bol,sun}}{2.5})} L_0 E_{ref}(\lambda, T) \frac{a_{pixel}}{a_{det}(\lambda)} \frac{\lambda}{hc} \frac{\pi A^2}{4} \varepsilon_{spect}(\lambda) C_{FRD} \mathrm{e}^- / \mathrm{sec} \tag{7.10}$$

In order to put this equation to use, the value of N must be found in terms of stellar spectral class and apparent visual magnitude, m_v.

The apparent bolometric magnitude is found from $m_{bol} = m_v + C_{BC}$, where both C_{BC} and the effective temperature, T, are directly related to the spectral classification. A value for λ must now be found to maximise N for each value of T (corresponding to the main spectral classifications).

By expanding equation 7.10 it can be seen that:

$$N_{pixel}(\lambda) \propto \frac{\varepsilon_{spect}(\lambda)}{\lambda^3} \left(e^{\frac{hc}{\lambda kT}} - 1 \right)^{-1} \tag{7.11}$$

This is shown graphically in Figure 7.7 for a number of stellar types.

Using the values for a 1meter / f8 telescope it is possible to calculate the peak values of N_{pixel} for a range of stellar types and magnitudes. For telescopes of other apertures, A, and f-ratios, the values from Table 7.1 used to find N_{pixel} by:

$$N_{pixel} = N_{\text{Table 7.1}} \times A^2 \times C_{FRD} \tag{7.12}$$

where C_{FRD} is from Figure 7.6 in the previous section of this chapter.

In addition to these “desired" electrons there are also a couple of noise sources which must be considered when using CCD detectors. The first of these is the readout noise, R. As the name suggests this is generated during the process of reading the CCD pixels. Although small, with a typical value being in the order of 100 electrons / pixel, (20 of less for a good CCD camera) cooling does little to lower the readout noise since the noise is proportional to the square root of the temperature.

The other major source of noise is the “dark" current , D. At room temperature, thousands of electrons per pixel per second are generated by thermal

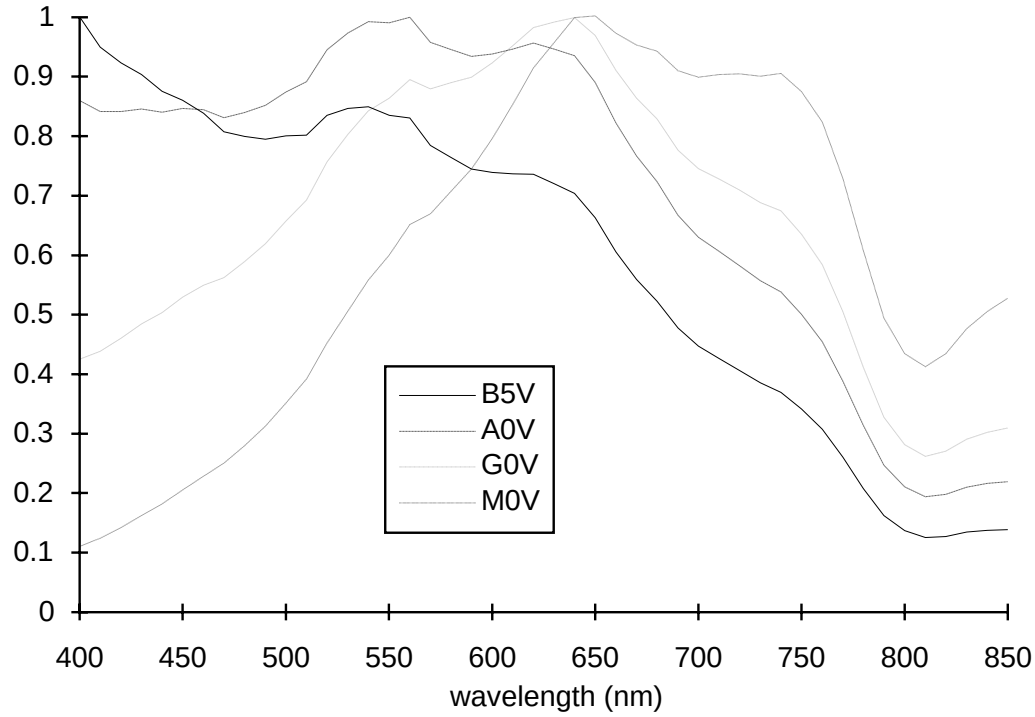

Figure 7.7: Pixel charge rate as a function of wavelength for a number of stellar types.

processes. Fortunately this process is exponentially dependant on temperature with a 7 degree (typically) reduction in temperature resulting in the dark current being reduced by a factor of 2.

From Genet et al. [1989] the signal to noise ratio, SNR, can be found from:

$$SNR = \frac{N_{pixel}\, t}{\sqrt{R^2 + \left(D + N_{pixel}\right) t}} \tag{7.13}$$

For a given detector, however, there is a maximum number of electrons that can accumulate in each pixel, M. This is commonly called the “well depth" of the detector. To avoid saturation then:

$$\left(D + N_{pixel}\right) t < M \tag{7.14}$$

The proposed detector, a TC215 CCD image sensor by Texas Instruments,

Table 7.1: Peak value of N_{pixel} (electrons / second / pixel) for a telescope with 1 metre aperture.

Class	**m_v=0**	**m_v=2.5**	**m_v=5**	**m_v=7.5**	**m_v=10**
O5	9.5E+04	9.5E+03	9.5E+02	9.5E+01	9.5E+00
O8	8.1E+04	8.1E+03	8.1E+02	8.1E+01	8.1E+00
B0	8.4E+04	8.4E+03	8.4E+02	8.4E+01	8.4E+00
B5	9.6E+04	9.6E+03	9.6E+02	9.6E+01	9.6E+00
B8	7.0E+04	7.0E+03	7.0E+02	7.0E+01	7.0E+00
A0	7.6E+04	7.6E+03	7.6E+02	7.6E+01	7.6E+00
A5	7.7E+04	7.7E+03	7.7E+02	7.7E+01	7.7E+00
A7	7.9E+04	7.9E+03	7.9E+02	7.9E+01	7.9E+00
F0	8.6E+04	8.6E+03	8.6E+02	8.6E+01	8.6E+00
F5	9.5E+04	9.5E+03	9.5E+02	9.5E+01	9.5E+00
F7	9.7E+04	9.7E+03	9.7E+02	9.7E+01	9.7E+00
G0	1.0E+05	1.0E+04	1.0E+03	1.0E+02	1.0E+01
G5	1.1E+05	1.1E+04	1.1E+03	1.1E+02	1.1E+01
G8	1.1E+05	1.1E+04	1.1E+03	1.1E+02	1.1E+01
K0	1.1E+05	1.1E+04	1.1E+03	1.1E+02	1.1E+01
K5	1.6E+05	1.6E+04	1.6E+03	1.6E+02	1.6E+01
K7	1.9E+05	1.9E+04	1.9E+03	1.9E+02	1.9E+01
M0	2.4E+05	2.4E+04	2.4E+03	2.4E+02	2.4E+01
M5	6.9E+05	6.9E+04	6.9E+03	6.9E+02	6.9E+01
M8	1.7E+06	1.7E+05	1.7E+04	1.7E+03	1.7E+02

has the following properties at 25°C:

$$\begin{aligned} D &\approx 20 \times 10^3 \text{ electrons / pixel / second} \\ M &\approx 60 \times 10^3 \text{ electrons / pixel} \\ R &\approx 60 \text{ electrons / pixel} \end{aligned}$$

Substituting these values into equations 7.13 & 7.14, then: for a SNR better than 100:

$$SNR > 100 \quad \Longrightarrow \quad N_{pixel} > 0.73D \tag{7.15}$$

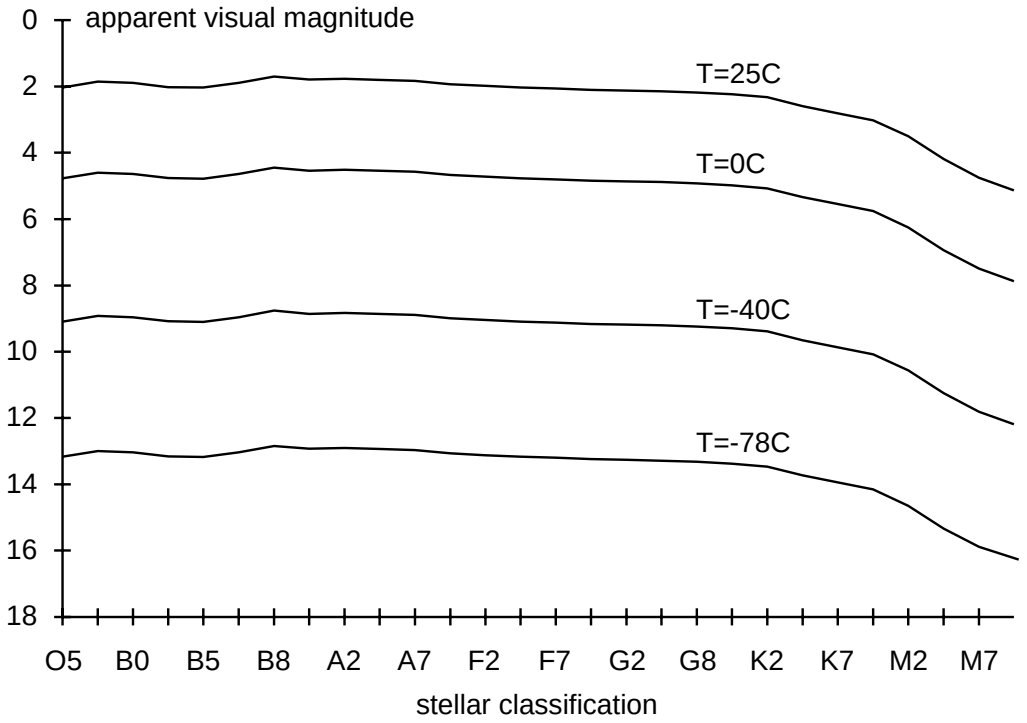

Figure 7.8: The limiting magnitudes for a range of stellar types at a number of CCD temperatures (1m / f8 telescope).

Once D is known the limiting magnitudes for a range of stellar types at a number of CCD temperatures can be calculated and are shown in Figure 7.8.

From equations 7.14 and 7.15 the exposure times for objects with $N_{pixel} \approx D$ (the dimmest objects that can be observed) is:

$$t = \frac{35 \times 10^3}{N_{pixel}} \tag{7.16}$$

For $N_{pixel} \gg D$ then for a $SNR > 100$ and no saturation of pixels the range of exposure times is:

$$\frac{8 \times 10^3}{N_{pixel}} < t < \frac{60 \times 10^3}{N_{pixel}} \tag{7.17}$$

This is illustrated in Figure 7.9. Note that at the upper limit of t a SNR of better than 230:1 should be possible.

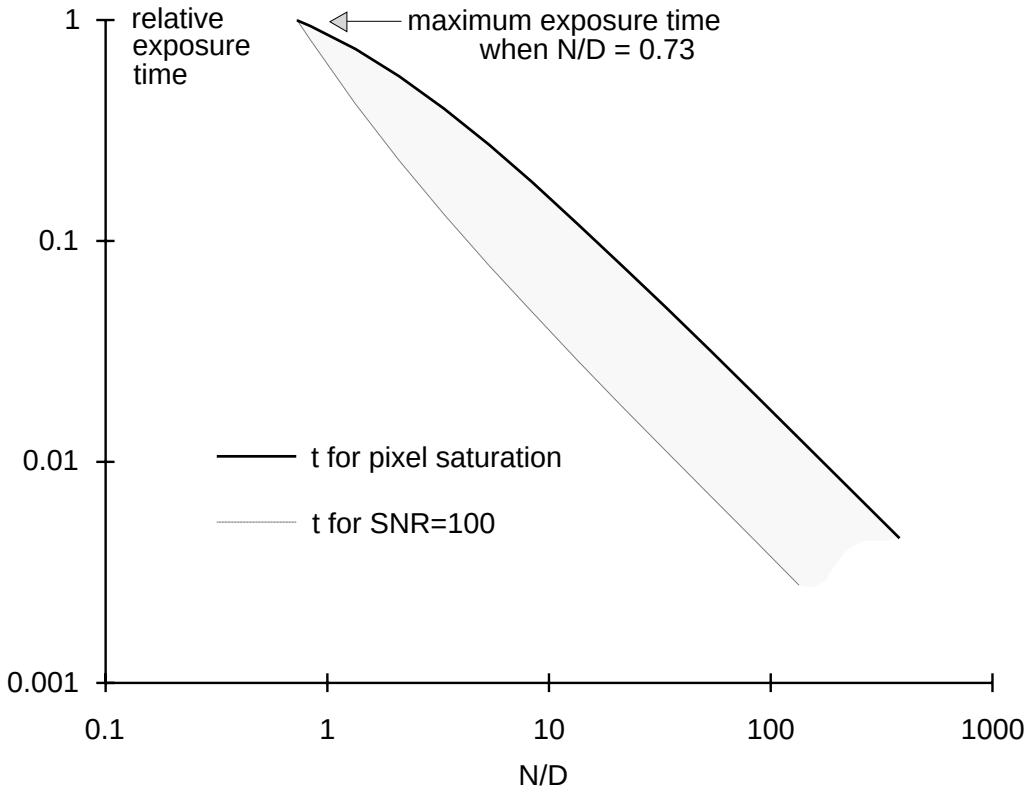

Figure 7.9: Relative exposure times as a function of the ratio N/D.

In order to quantify these results a brief comparison with other spectrographs will be made assuming the use of a similar sized telescope. From earlier in this chapter the resolving power is of this spectrograph (UQES) is expected to be 15,000 at a maximum efficiency of 20%.

MUSICOS [Baudrand and Böhm, 1992]:

- Fibre fed echelle spectrograph
- Resolving power 35000 using 2 exposures.
- Thompson CCD detector with 20μ square pixels
- Exposure time for $m_v = 7$, A0V star $\approx$ 60min @ $SNR < 400$ using a 2m telescope
- UQES: exposure time $\approx$ 3min @ $SNR < 230$.

NOTE The larger SNR and resolving power largely accounts for the factor of 20 increase in exposure time for MUSICOS.

Hamilton Echelle [Vogt, 1987]:

- Coudé mounted echelle spectrograph
- Resolving power 30000 over a 2000Å to 5000Å range.
- TI 800×800 CCD.
- Exposure time for $m_v = 12.3 \approx 30\text{min}$ @ $SNR \approx 150$ using a 3m telescope
- UQES: exposure time $\approx 50\text{min}$ @ $SNR < 150$

Kitt Peak National Observatory (measurements by Nations and Seeds [1986])

- Coudé spectrograph - not echelle type.
- 175Å per exposure @ 0.5Å resolution.
- TI CCD detector.
- Exposure time for $mv = 7.3$, G8IV star $< 60\text{min}$ (36" telescope)
- UQES exposure time $< 8\text{min}$ for complete visible range.

Clearly once the various design parameters are taken into account the expected performance of UQES is on par with other similar instruments. The comparison with the coudé spectrograph at Kitt Peak clearly shows the significant performance advantages of an echelle type spectrograph over traditional grating spectrograph designs.

While still on the subject of exposure times it is valuable to estimate the performance of UQES on a sample of the objects for which this spectrograph was designed to measure. As mentioned in the introduction the spectroscopic properties of irregular variables, in particular Be type stars, are of particular interest. The following table gives approximate exposure times for both 1 metre and Celestron^{TM} C14 (0.35m) telescopes.

Table 7.2: Exposure times for some Be type stars for telescopes with 1 metre and 0.35 metre apertures.

Name	**Type**	**V mag**	**t(1m)**	t(C14)
Alf Eri	B4Ve	0.5	0.7sec	6sec[1]
Eta Cen	B2IVe	2.31	3.5sec[1]	30sec[2]
Alf Col	B7IVe	2.6	5sec[1]	40sec[2]
Alf Ara	B3Ve	3	7sec[1]	1min[2]
Bet Pic	A5IVsh	3.8	15sec[1]	2min[2]
Lam Pav	B1.5IIIe	4.22	20sec[2]	3min[3]
Bet Mon A	B4Ve sh	4.6	30sec[2]	4min[3]
56 Eri	B2Ve	5.9	1.5min[2]	13min[3]
MWC304	B1Vnpe	7.81	10min[3]	1.5hr[4]

CCD maximum temperatures: *unmarked* = no cooling;
[1] = 0°C; [2] = -20°C; [3] = -40°C; [4] = -60°C